

Two-center basis generator method calculations for Li^{3+} , C^{3+} and O^{3+} ion impact on ground state hydrogen

Anthony C. K. Leung and Tom Kirchner*

*Department of Physics and Astronomy,
York University, Toronto, Ontario, M3J 1P3, Canada*

(Dated: December 28, 2021)

Abstract

The two-center basis generator method is used to obtain cross sections for excitation, capture, and ionization in Li^{3+} , C^{3+} , and O^{3+} collisions with ground-state hydrogen at projectile energies from 1 to 100 keV/u. The interaction of the C^{3+} and O^{3+} projectiles with the active electron is represented by a model potential. Comparisons of cross sections with previously reported data show overall good agreement while discrepancies in capture for C^{3+} collisions at low energies are noted. The present results show that excitation and ionization are similar across the three collision systems, which indicates that these cross sections are mostly dependent on the net charge of the projectile only. The situation is different for the capture channel.

I. INTRODUCTION

Collisions between partially-stripped ions and neutrals (atoms or molecules) are more commonly found in nature than collisions with bare ions. Partially-stripped ion collisions have been a subject of interest in astrophysical [1, 2] and plasma applications [3], and thus, interest in accurate cross sections for electronic processes in these collisions remains high. In recent times, the International Nuclear Data Committee within the International Atomic Energy Agency has expressed interest in cross sections from collisions between bare or partially-stripped projectiles with atomic hydrogen, which are necessary for neutral beam modeling in fusion plasma [4].

In this study, new calculated cross sections for collision systems involving ground-state hydrogen and ions of net charge $Q = 3$ are reported. Specifically, the projectile ions Li^{3+} , C^{3+} and O^{3+} are chosen for this analysis. Cross sections for electron excitation, capture, and ionization are compared with data that are available in the literature. Currently, there is a broad coverage of cross sections for Li^{3+} -H(1s) collisions from the low to the high energy regimes (e.g., References [5–7]). Although data exist for C^{3+} and O^{3+} collisions with atomic hydrogen [8–10], there are some gaps for excitation and ionization data in the intermediate energy regime. Therefore, the objectives of this study are to report cross sections in these gaps, perform validity checks on existing ones, and provide a comparison for the three ions to throw light on the question to which extent the net charge alone determines the cross sections.

The approach used in the present theoretical analysis is the semiclassical, nonperturbative

* tomk@yorku.ca

two-center basis generator method (TC-BGM) [11]. As a close-coupling approach, the main feature of the TC-BGM is its use of a dynamical basis that is adapted to the problem at hand, which provides a practical advantage in terms of reaching convergence with smaller basis sets than required in standard approaches. Relevant to this study, the TC-BGM was used before in References [12, 13] to obtain accurate capture and ionization cross sections for Li^{3+} -H(1s) collisions at impact energies of 10 keV/u and higher. The present work focuses on collisions at impact energies from 1 to 100 keV/u.

The article is organized as follows. In Section II, an overview of the TC-BGM for ion-atom collisions is given. In Section III, cross sections for the three collision systems are presented and discussed. Finally in Section IV, concluding remarks are provided. Atomic units ($\hbar = e = m_e = 4\pi\epsilon_0 = 1$) are used throughout the article unless stated otherwise.

II. THEORETICAL METHOD

The focus of this study is on collisions in the low- and intermediate-impact energy regimes, specifically from 1 to 100 keV/u. The collisional framework used here is based on the impact-parameter model within the semiclassical approximation. Such a framework to solve the time-dependent Schrödinger equation (TDSE) with the TC-BGM has been used in previous studies and has also been described at length in a prior work related to collisions with atomic hydrogen [14]. For this reason, only a summary highlighting the core ideas and some details regarding the potentials used are given.

In the laboratory frame, the hydrogen target is assumed to be fixed in space and the projectile ion travels in a straight-line path at constant speed v_P , described by $\mathbf{R}(t) = (b, 0, v_P t)$, where b is the impact parameter. The objective is to solve the TDSE for the initially occupied ground state in the target,

$$i\frac{\partial}{\partial t}\psi(\mathbf{r}, t) = \hat{h}(t)\psi(\mathbf{r}, t). \quad (1)$$

For the present study, the projectile ions under consideration are Li^{3+} , C^{3+} , and O^{3+} . This study assumes that the strongly bound electrons in the C^{3+} and O^{3+} ions remain frozen during the collision. This allows the single-particle Hamiltonian to be decomposed as

$$\hat{h}(t) = -\frac{1}{2}\nabla^2 + V_T(|\mathbf{r}|) + V_P(|\mathbf{r}_P|, t), \quad (2)$$

where \mathbf{r}_P is the electron position vector with respect to the projectile and is related to that with respect to the target by $\mathbf{r}_P(t) = \mathbf{r} - \mathbf{R}(t)$. The projectile Li^{3+} is represented by the Coulomb potential with $Z_P = 3$. For the C^{3+} projectile, two sets of cross sections are produced where one is generated using the optimized potential model (OPM) [15] and another one using a screened Coulomb potential based on the Green, Sellin, and Zachor (GSZ) model [16]. The potential for the O^{3+} projectile is represented with the GSZ model. Numerical parameters to obtain GSZ potentials for C^{3+} and O^{3+} are taken from Szydlik and Green [17].

The TDSE (1) is solved by projection onto a finite set of basis states and propagation using the TC-BGM. The basis sets that were used for this analysis include: all nlm states from $n = 1$ to $n = 5$ of the hydrogen target, states from $n = 1$ to $n = 6$ of Li^{2+} , states from $n = 2$ to $n = 6$ of C^{2+} and O^{2+} ions, and 45 BGM pseudostates to account for intermediate quasimolecular couplings and ionization to the continuum. Bound-state probabilities for finding the electron on the target p^{tar} or on the projectile p^{cap} are calculated from summing up the transition probabilities within the bound-state basis sets, and probabilities for total ionization p^{ion} are obtained from the unitarity criterion

$$p^{\text{ion}} = 1 - p^{\text{tar}} - p^{\text{cap}}. \quad (3)$$

Finally, cross sections for the electronic transitions are obtained by integrating the probabilities over the impact parameter

$$\sigma = 2\pi \int_0^{b_{\max}} bp(b)db, \quad (4)$$

where b_{\max} (in a.u.) is the upper bound at which the integral is cut in practice. For the collision calculations reported here, an upper bound of $b_{\max} = 20$ a.u. was more than sufficient to capture the asymptotic profile of these transition probabilities. It should also be noted that the conservation of unitarity (3) was monitored in the present analysis and it was found that deviations produced by the calculations are typically no larger than 1%.

III. RESULTS AND DISCUSSION

A. $\text{Li}^{3+}\text{-H(1s)}$

Cross section results for the $\text{Li}^{3+}\text{-H(1s)}$ collision system are shown in Figure 1. Starting with the n -state excitation cross sections (Fig. 1a), the present TC-BGM results are compared with other calculations. The work by Suarez *et al.* [18] reported recommended excitation cross sections based on the two-center one-electron diatomic molecule expansion covering 1 to 80 keV/u and the one-center Bessel expansion that covers energies greater than 80 keV/u. The work by Agueny *et al.* [19] was based on the two-center atomic orbital close-coupling method with Gaussian-type orbitals (TC-AOCC-GTO). Only excitation of the $n = 2$ and $n = 3$ shells are presented, since transition to higher energy states are not important at these impact energies [18]. It is shown that the present TC-BGM results are in satisfactory agreement with previously reported cross sections [18, 19].

In Figure 1b, total electron capture cross sections for the $\text{Li}^{3+}\text{-H(1s)}$ collision system are shown. The present TC-BGM capture results show an impact-energy dependence, which is consistent with previously reported results, namely, the TC-AOCC-GTO [19], another TC-AOCC-GTO calculation by Toshima [20], and the advanced adiabatic method by Janev *et al.* [21]. Quantitatively, the present cross sections are closest to the TC-AOCC-GTO results [19, 20] at all impact energies. There are some differences in the advanced adiabatic calculations [21] compared with the present results but they are no more than 20%, and smaller at low energies where the advanced adiabatic method [21] is expected to work best.

Figure 1c shows the ionization results for $\text{Li}^{3+}\text{-H(1s)}$ collisions. The present cross sections are compared with those from the advanced adiabatic [21] and TC-AOCC-GTO [19, 20] calculations. It can be seen that the present TC-BGM results are consistent with the previous calculations and show that ionization is important in the intermediate energy regime at 10 keV/u and above but negligible at lower energies. They are also consistent with the aforementioned studies [12, 13] using the TC-BGM on $\text{Li}^{3+}\text{-H(1s)}$ collisions at 10 keV/u and above. Overall, the cross sections produced by the TC-BGM are in good agreement with previous calculations.

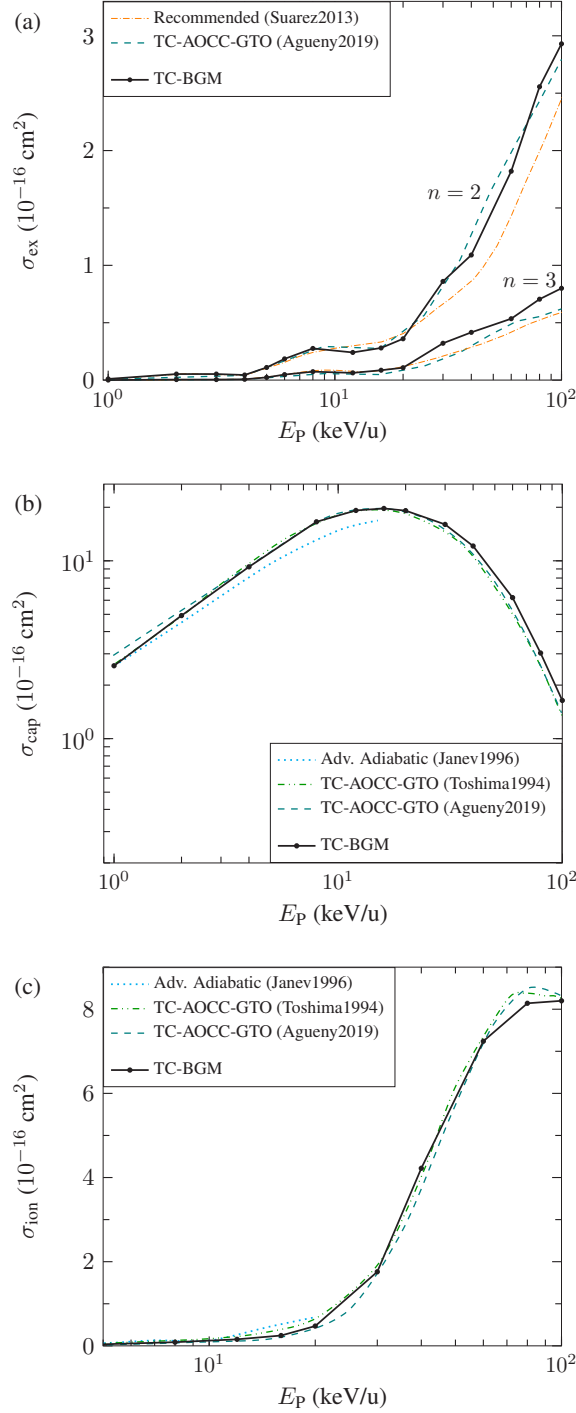


FIG. 1. Cross sections of (a) target-excitation, (b) electron capture, and (c) ionization for Li³⁺-H(1s) collisions from 1 to 100 keV/u. Recommended data from Ref. [18]. Theory: present TC-BGM, TC-AOCC-GTO [19, 20], and Advanced Adiabatic [21].

B. C³⁺-H(1s)

Shown in Figure 2 are the cross section results for C³⁺ collisions with ground-state hydrogen. The n -state excitation cross sections in Figure 2a only include results from the present TC-BGM calculations since, to our knowledge, no other results are available in the literature. Two sets of results from TC-BGM calculations are shown where one set is based on using the OPM to represent the partially-stripped ion and the other set is based on the GSZ potential. The excitation cross sections show the typical increasing behavior as impact energy increases. There are some discrepancies between the OPM and GSZ results around 100 keV/u but those differences decrease towards lower energies. Similar to Li³⁺ collisions, the dominant excitation channel in the C³⁺-H(1s) system is $n = 2$ followed by $n = 3$. One can also see the qualitative and quantitative similarities in the cross section profiles of these two systems with excitation processes being important at 20 keV/u and higher. This observation reflects the fact that the target electron mainly experiences an overall net charge of $Q = 3$ (i.e., same as for Li³⁺ impact) and that other interactions are of minor importance.

In Figure 2b, total capture cross sections for C³⁺-H(1s) collisions are presented. Again, two sets of TC-BGM results are shown where one set is based on using the OPM for the projectile while the other one is based on the GSZ potential. Shown alongside with the present cross sections are previously reported values from calculations using a molecular-orbital close-coupling (MOCC) scheme [9], calculations using an AOCC expansion [22], calculations based on the electron nuclear dynamics (END) approach [10], and a set of recommended values based on theoretical and experimental works compiled by Janev *et al.* [8] with a 25% uncertainty band. Both the MOCC calculation [9] and the AOCC calculation [8] are explicit two-electron calculations. One can see that the TC-BGM cross sections at low energies are significantly lower than the previously reported results. Between the two sets of the present TC-BGM results the capture cross section produced from using the GSZ potential is slightly closer to previous results than that obtained from using the OPM. The discrepancies at low energies could be due to the present treatment of the C³⁺ projectile, which assumes that the screening of the nucleus is frozen throughout the course of the collision. Interestingly, the differences in capture between the OPM and GSZ results decrease as impact energy increases; the opposite tendency as seen for excitation (Fig. 2a).

The overall agreement of the present TC-BGM ionization cross sections with the recom-

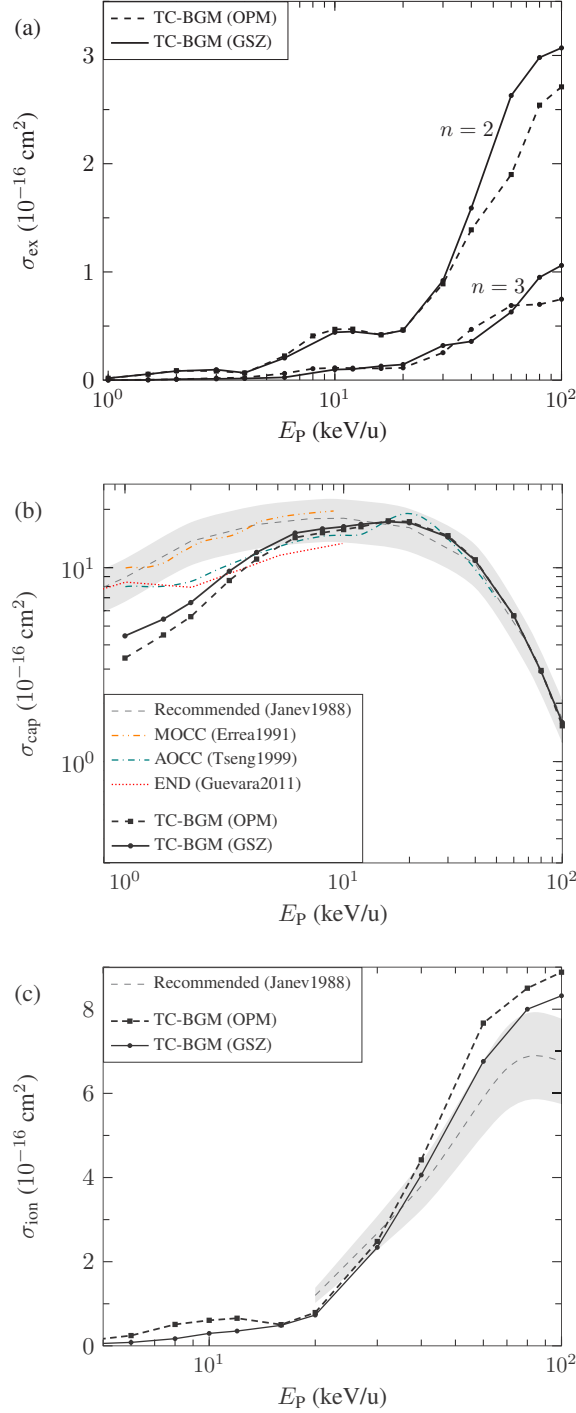


FIG. 2. Cross sections for C^{3+} -H(1s) collisions from 1 to 100 keV/u: (a) target-excitation; (b) electron capture; (c) ionization. Recommended data from Ref. [8]. Theory: present TC-BGM, MOCC [9], AOCC [22], and END [10].

mended values [8] shown in Figure 2c is satisfactory. The cross section profile from the present calculations shows the expected behavior where ionization is not important at 10 keV/u and below. At higher energies one can see the typical profile of an increasing cross section. One can also see the quantitative similarities of Li^{3+} and C^{3+} impact between 10 and 100 keV/u. Overall, it appears that the present cross section calculated using the GSZ potential is closer to the recommended values than the results that are based on the OPM.

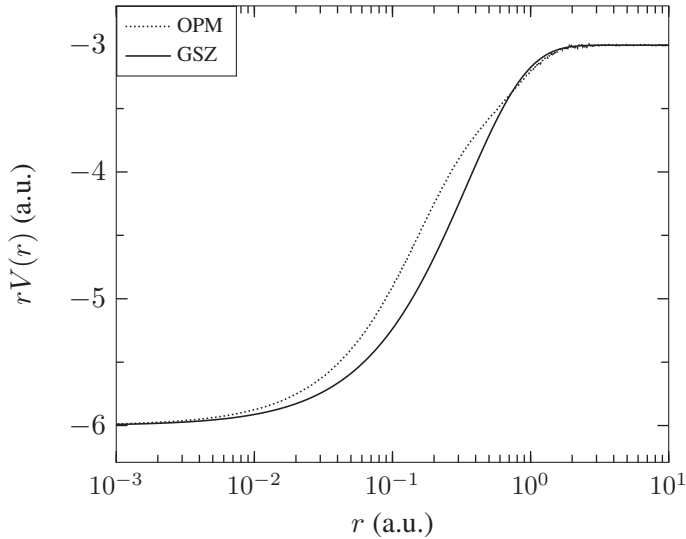


FIG. 3. Distance-weighted effective potential of the C^{3+} projectile as a function of radial distance. Potentials calculated using the OPM [15] and GSZ [17] are displayed.

Figure 3 illustrates the differences between the OPM and the GSZ potentials, where the r -weighted potentials are plotted with respect to the radial distance. The potential profiles show identical asymptotic behaviors at short and long distances but display some differences in the $r \in [0.01, 1]$ a.u. interval where the GSZ potential is mostly lower than the OPM. In other words, the GSZ models a potential that is more attractive than the OPM.

C. O^{3+} -H(1s)

Figure 4 shows the set of cross sections for O^{3+} -H(1s) collisions. The excitation cross sections in Figure 4a show the typical increasing behavior between 1 and 100 keV/u. Moreover, one can again see that the dominant channel is $n = 2$ and the quantitative similarities to the results for Li^{3+} and C^{3+} collisions. Specifically, a cross section value of approximately $3 \times 10^{-16} \text{ cm}^2$ for

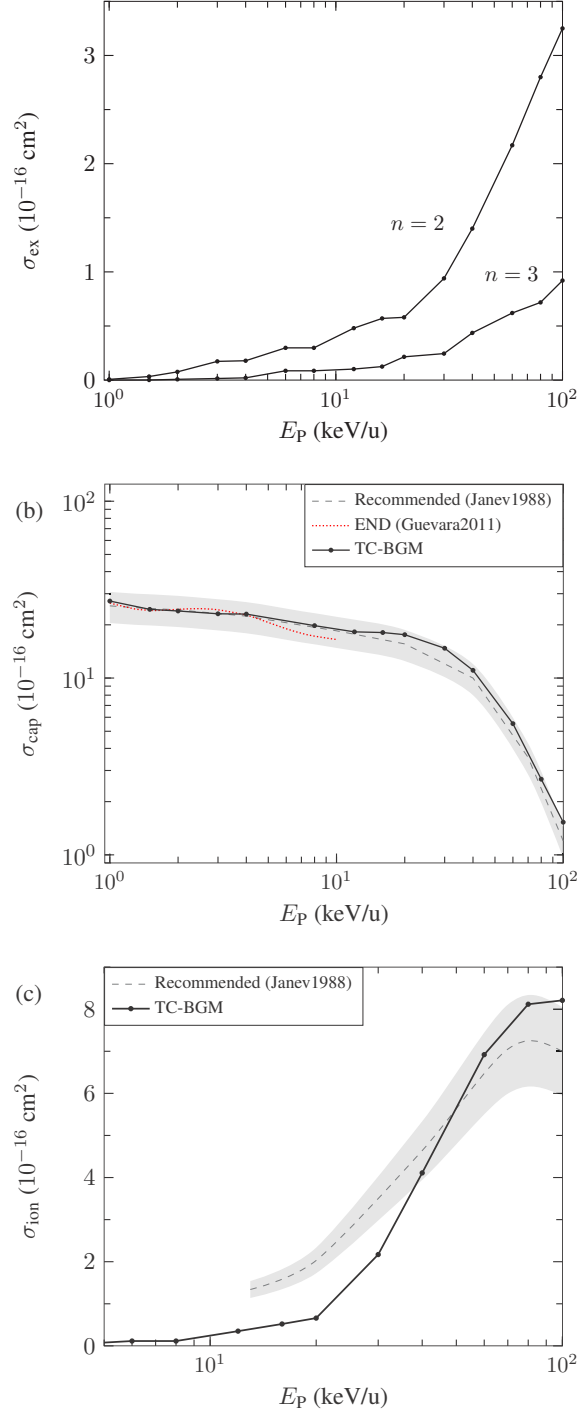


FIG. 4. Cross sections for O^{3+} -H collisions from 1 to 100 keV/u: (a) target-excitation; (b) electron capture; (c) ionization. Recommended data from Ref. [8]. Theory: present TC-BGM and END [10].

the $n = 2$ channel is obtained at 100 keV/u across all three collision systems.

In Figure 4b, total capture cross sections calculated from the present TC-BGM are compared with the previously reported recommended values [8] and the more recent results from END calculations [10]. The present results are quantitatively consistent with the previous results and are within the uncertainty range of the recommended values [8]. This is in contrast to the observation that was made for the capture cross section in C^{3+} collisions (Figure 2b) where discrepancies with the END and with other calculations are significant at low impact energies. In addition, the capture profile here is noticeably different from that of the Li^{3+} (Figure 1b) and C^{3+} (Figure 2b) collisions, with capture by O^{3+} ions showing a monotonic decrease over the entire energy range displayed.

Figure 4c shows the total ionization cross section. The present TC-BGM results are compared with the previously compiled recommended values [8]. One can see that the present results are well within the uncertainty range of the recommended values between 40 and 100 keV/u but fall short at lower energies. Given that only these recommended values are available, additional independent studies are necessary to provide further validation of the present results.

IV. CONCLUSIONS

In this work, we reported TC-BGM cross section calculations for Li^{3+} , C^{3+} , and O^{3+} collisions with ground-state hydrogen from 1 to 100 keV/u. Cross sections for electron excitation, capture, and ionization were obtained for all three systems. Overall, we found satisfactory agreement between the present cross sections and previously reported values.

We also drew a few comparisons of the cross sections across the different projectiles. This is summarized in Figure 5 where total cross sections for excitation, capture, and ionization for all three collision systems are plotted together. One can observe the similarities in the energy dependence of the excitation and ionization cross sections across the three systems. For capture, differences in cross sections are significant at 10 keV/u and below, indicating that the precise form of the screening of the projectile nucleus matters.

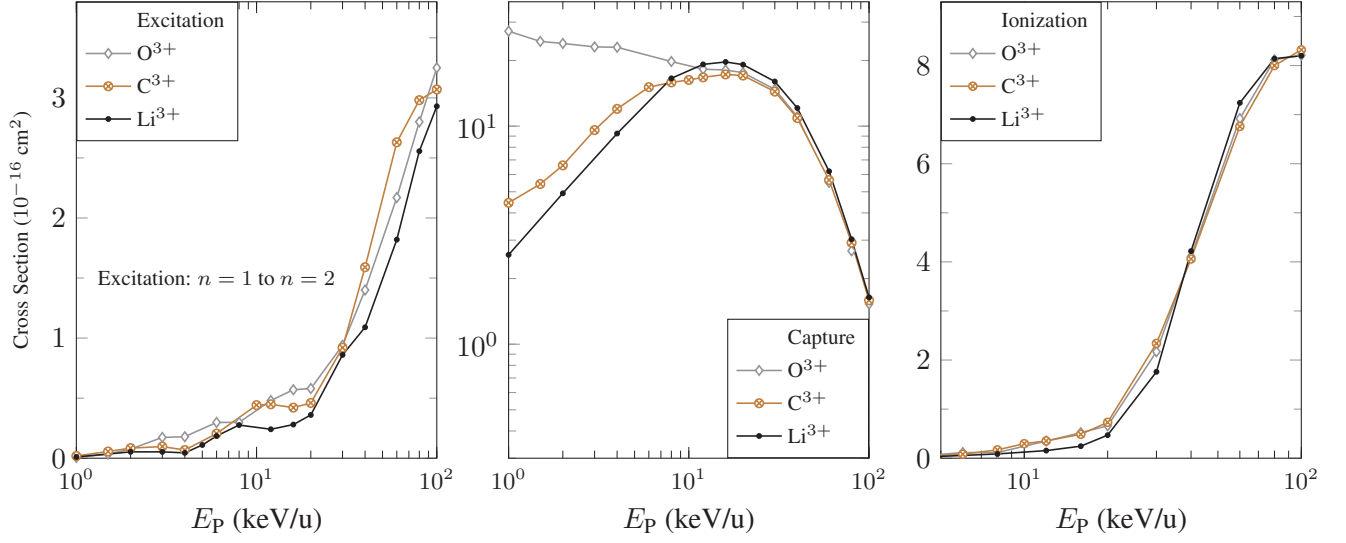


FIG. 5. TC-BGM cross sections of Li^{3+} -, C^{3+} -, and O^{3+} -H(1s) collisions plotted with respect to impact energies for target-excitation from $n = 1$ to $n = 2$ (left panel), total electron capture (middle panel), and total ionization (right panel).

ACKNOWLEDGMENTS

Financial support from the Natural Sciences and Engineering Research Council of Canada (NSERC) (RGPIN-2019-06305) is gratefully acknowledged. This work was made possible with the high-performance computing resources provided by Compute/Calcul Canada.

APPENDIX

The cross section data from the TC-BGM calculations for Li^{3+} , C^{3+} , and O^{3+} collisions with ground-state hydrogen are presented in Tables I, II, and III. For the C^{3+} and O^{3+} projectiles the GSZ potential has been used.

TABLE I. n -state selective excitation cross sections (10^{-16} cm 2) for Li $^{3+}$, C $^{3+}$, and O $^{3+}$ collisions with ground-state hydrogen from 1 to 100 keV/u.

| E(keV/u) | Li $^{3+}$ -H(1s) | | C $^{3+}$ -H(1s) | | O $^{3+}$ -H(1s) | |
|----------|-------------------|-------|------------------|-------|------------------|--------|
| | n=2 | n=3 | n=2 | n=3 | n=2 | n=3 |
| 1 | 0.010 | 0.001 | 0.019 | 0.001 | 0.007 | <0.001 |
| 2 | 0.053 | 0.005 | 0.084 | 0.009 | 0.076 | 0.007 |
| 3 | 0.053 | 0.005 | 0.097 | 0.012 | 0.173 | 0.015 |
| 4 | 0.045 | 0.007 | 0.068 | 0.016 | 0.179 | 0.021 |
| 6 | 0.185 | 0.048 | 0.205 | 0.026 | 0.298 | 0.086 |
| 8 | 0.276 | 0.074 | 0.442 | 0.098 | 0.341 | 0.071 |
| 12 | 0.241 | 0.063 | 0.449 | 0.102 | 0.480 | 0.102 |
| 16 | 0.280 | 0.086 | 0.421 | 0.130 | 0.570 | 0.125 |
| 20 | 0.360 | 0.108 | 0.460 | 0.145 | 0.580 | 0.215 |
| 30 | 0.860 | 0.321 | 0.920 | 0.320 | 0.940 | 0.245 |
| 40 | 1.090 | 0.416 | 1.590 | 0.358 | 1.400 | 0.436 |
| 60 | 1.820 | 0.535 | 2.630 | 0.630 | 2.170 | 0.620 |
| 80 | 2.556 | 0.705 | 2.981 | 0.950 | 2.800 | 0.718 |
| 100 | 2.930 | 0.800 | 3.070 | 1.060 | 3.250 | 0.920 |

TABLE II. Total-capture cross sections (10^{-16} cm 2) for Li $^{3+}$, C $^{3+}$, and O $^{3+}$ collisions with ground-state hydrogen from 1 to 100 keV/u.

| E(keV/u) | Li $^{3+}$ -H(1s) | C $^{3+}$ -H(1s) | O $^{3+}$ -H(1s) |
|----------|-------------------|------------------|------------------|
| 1 | 2.57 | 4.45 | 27.26 |
| 2 | 4.92 | 6.61 | 23.95 |
| 3 | 7.24 | 9.59 | 23.09 |
| 4 | 9.25 | 12.00 | 23.00 |
| 6 | 13.86 | 15.10 | 21.10 |
| 8 | 16.57 | 15.87 | 19.79 |
| 12 | 19.20 | 16.74 | 18.25 |
| 16 | 19.70 | 17.27 | 18.09 |
| 20 | 19.15 | 17.06 | 17.59 |
| 30 | 16.02 | 14.40 | 14.74 |
| 40 | 12.11 | 10.89 | 11.06 |
| 60 | 6.21 | 5.66 | 5.52 |
| 80 | 3.03 | 2.92 | 2.68 |
| 100 | 1.64 | 1.59 | 1.53 |

TABLE III. Total-ionization cross sections (10^{-16} cm 2) for Li $^{3+}$, C $^{3+}$, and O $^{3+}$ collisions with ground-state hydrogen from 1 to 100 keV/u.

| E(keV/u) | Li $^{3+}$ -H(1s) | C $^{3+}$ -H(1s) | O $^{3+}$ -H(1s) |
|----------|-------------------|------------------|------------------|
| 1 | < 0.001 | 0.002 | 0.001 |
| 2 | 0.003 | 0.011 | 0.007 |
| 3 | 0.006 | 0.026 | 0.030 |
| 4 | 0.014 | 0.028 | 0.034 |
| 6 | 0.042 | 0.082 | 0.115 |
| 8 | 0.087 | 0.172 | 0.115 |
| 12 | 0.155 | 0.352 | 0.350 |
| 16 | 0.245 | 0.487 | 0.502 |
| 20 | 0.466 | 0.731 | 0.660 |
| 30 | 1.760 | 2.340 | 2.173 |
| 40 | 4.215 | 4.056 | 4.019 |
| 60 | 7.236 | 6.757 | 6.811 |
| 80 | 8.141 | 8.003 | 8.118 |
| 100 | 8.198 | 8.320 | 8.209 |

- [1] T. E. Cravens, *Astrophys. J.* **532**, L153 (2000).
- [2] O. Abu-Haija, J. A. Wardwell, and E. Y. Kamber, *J. Phys. Conf. Ser.* **58**, 195 (2007).
- [3] H. Bruhns, H. Kreckel, D. W. Savin, D. G. Seely, and C. C. Havener, *Phys. Rev. A* **77**, 064702 (2008).
- [4] H.-K. Chung, *Data for Atomic Processes of Neutral Beams in Fusion Plasma Summary Report of the First Revision* Tech. Rep. (International Atomic Energy Agency (IAEA), 2017).
- [5] M. B. Shah, T. V. Goffe, and H. B. Gilbody, *J. Phys. B* **11**, 2 (1978).
- [6] W. Fritsch and C. D. Lin, *J. Phys. B* **15**, L281 (1982).
- [7] I. Murakami, J. Yan, H. Sato, M. Kimura, R. K. Janev, and T. Kato, *At. Data Nucl. Data Tables* **94**, 161 (2008).
- [8] R. Janev, R. Phaneuf, and H. Hunter, *At. Data Nucl. Data Tables* **40**, 249 (1988).
- [9] L. F. Errea, B. Herrero, L. Méndez, O. Mó, and A. Riera, *J. Phys. B* **24**, 4049 (1991).
- [10] N. L. Guevara, E. Teixeira, B. Hall, Y. Öhrn, E. Deumens, and J. R. Sabin, *Phys. Rev. A* **83**, 052709 (2011).
- [11] M. Zapukhlyak, T. Kirchner, H. J. Lüdde, S. Knoop, R. Morgenstern, and R. Hoekstra, *J. Phys. B* **38**, 2353 (2005).
- [12] H. J. Lüdde, T. Kalkbrenner, M. Horbatsch, and T. Kirchner, *Phys. Rev. A* **101**, 062709 (2020).
- [13] H. J. Lüdde, A. Jorge, M. Horbatsch, and T. Kirchner, *Atoms* **8**, 10.3390/ATOMS8030059 (2020).
- [14] A. C. K. Leung and T. Kirchner, *Eur. Phys. J. D* **73**, 246 (2019).
- [15] E. Engel and S. H. Vosko, *Phys. Rev. A* **47**, 2800 (1993).
- [16] A. E. S. Green, D. L. Sellin, and A. S. Zachor, *Phys. Rev.* **184**, 1 (1969).
- [17] P. P. Szydlik and A. E. Green, *Phys. Rev. A* **9**, 1885 (1974).
- [18] J. Suarez, F. Guzman, B. Pons, and L. F. Errea, *J. Phys. B* **46**, 10.1088/0953-4075/46/9/095701 (2013).
- [19] H. Agueny, J. P. Hansen, A. Dubois, A. Makhoute, A. Taoutioui, and N. Sisourat, *At. Data Nucl. Data Tables* **129-130**, 101281 (2019).
- [20] N. Toshima, *Phys. Rev. A* **50**, 3940 (1994).
- [21] R. K. Janev, E. A. Solov'ev, and Y. Wang, *J. Phys. B* **29**, 2497 (1996).
- [22] H. C. Tseng and C. D. Lin, *J. Phys. B* **32**, 5271 (1999).